Misincorporation by Wild-Type and Mutant T7 RNA Polymerases: Identification of Interactions That Reduce Misincorporation Rates by Stabilizing the Catalytically Incompetent Open Conformation†

Jianbin Huang, Luis G. Brieba, and Rui Sousa*

Department of Biochemistry, University of Texas Health Sciences Center, 7703 Floyd Curl Drive, San Antonio, Texas 78284-7760

Received March 14, 2000; Revised Manuscript Received May 17, 2000

ABSTRACT: We have characterized the misincorporation properties of wild-type (wt) T7 RNAP and of 45 T7RNAP point mutants. The wt enzyme selects strongly against incorporation of an incorrect nucleotide. From the measured rates of misincorporation, an average error frequency of 1 in 2×10^4 is estimated. RNAs bearing 3′-mismatches are extended more slowly than correctly paired 3′-termini, and mismatches one or two bases away from the RNA 3′-end can also slow extension severely even when the 3′-base is correctly paired. Though it has been reported that T7RNAP has a 3′ → 5′ nuclease activity, we were unable to detect any endogenous T7RNAP RNase activity in elongation complexes. Pyrophosphorolysis was detected but does not appear to contribute to proofreading. Therefore, unlike other RNAPs, T7RNAP fidelity appears to depend entirely on discrimination against incorporation of the incorrect nucleotide and not on post-misincorporation proofreading. Alanine substitution of the H784 side chain, which interacts with the 3′ RNA·template base pair, increases both misincorporation and mismatch extension, while substitutions at G640, F644, and G645 increase misincorporation, but not mismatch extension. The latter three amino acids are in a part of the RNAP which interacts with the templating base and with the base immediately 5′ to the templating base. Mutation of these amino acids not only increases misincorporation, but also eliminates pausing during promoter clearance. The effects of these mutations and the interactions observed in a crystal structure of a transcribing complex indicate that these mutations disrupt interactions which limit misincorporation rates by stabilizing the catalytically incompetent open conformation of the RNAP.

Fidelity in DNA replication, transcription, and translation is essential for life. The fidelity mechanisms of DNA synthesis and protein translation have been extensively studied (*1*). The mechanisms of transcriptional fidelity have received less attention, though the misincorporation and proofreading properties of *E. coli* RNAP (*2*) and eukaryotic RNAP II (*3*) have been characterized. T7RNAP is the best characterized representative of a widespread family of RNAPs that includes most phage-encoded RNAPs and the mitochondrial RNAPs (*4*). While T7RNAP has been otherwise extensively studied, its misincorporation properties have not been well characterized. However, with crystal structures of the T7RNAP apoenzyme (*5*) and of its complexes with promoter DNA (*6*), with a transcript (*7*), and with a regulatory protein (*8*) now available, this polymerase presents an excellent system in which to gain insights into the structural mechanisms of transcriptional fidelity.

Studies of replication and transcriptional fidelity have revealed a number of mechanisms used by polymerases to ensure faithful nucleic acid synthesis. On the basis of kinetic studies, it was proposed that during DNA synthesis a conformational change in the polymerase, from an 'open' to a 'closed' conformation, follows dNTP binding (*9*). Recent crystal structures of DNAPs complexed with template and substrates support this proposal, and show that the open conformation represents a catalytically incompetent state (*10*−*13*). They also indicate that the isomerization to the catalytically competent closed conformation involves movements in both the polymerase and template strand. Binding of correct (complementary) dNTPs is suggested to be better at inducing this isomerization than binding of incorrect dNTPs, so the open to closed isomerization is proposed to be a critical component of the fidelity mechanism of DNAPs (*13*). T7RNAP is homologous to the Pol I family of DNAPs (*14*), and has a similar catalytic mechanism (*15*), so it is of interest to determine whether this RNAP uses a similar open to closed isomerization to limit misincorporation.

In addition to having mechanisms that limit misincorporation, polymerases increase fidelity by removing bases from the primer or RNA after misincorporation has occurred. In DNAPs, this usually involves a separate exonucleolytic site on the polymerase which removes bases in a 3′ → 5′ fashion (*16*). *E. coli* RNAP and RNAP II have also been found to have a 3′ → 5′ RNase activity. It is as yet unclear if this activity is a property of the RNAP itself, or if it is attributable to the GreA/B (for *E. coli* RNAP) or SII (for RNAP II)

† Supported by NIH Grant GM 52522 (to R.S.) and by a Fulbright-CONACYT fellowship (to L.G.B.).

* To whom correspondence should be addressed. Phone: 210-567-8782; Fax: 210-567-8778; E-mail: sousa@biochem.uthscsa.edu.

10.1021/bi000579d CCC: $19.00
Published on Web 08/26/2000

transcription factors, but it is clearly stimulated by these factors (*17*, *18*). Preferential removal of incorrect vs correct bases from the RNA or primer may depend on a faster rate of removal of incorrect bases, as well as a slower rate of extension of mispaired termini which allows the exonucleolytic activity more time to act on mispaired vs correctly paired termini (*2*, *3*). It has been reported that T7RNAP has endogenous RNase activity (*19*), so we were also interested in determining if this activity would allow T7RNAP to proofread.

To address these questions, we have characterized the misincorporation properties of wt T7RNAP and of a large number of T7RNAP point mutants. We find that T7RNAP selects against incorporation of an incorrect base to a degree similar to that of highly accurate DNAPs such as DNAP I. Though we found that extension of mispaired termini was slower than extension of correctly paired termini, we were unable to detect any post-misincorporation proofreading activity in this enzyme. We identified a number of mutations that increased misincorporation rates. Interestingly, some of these mutations appear to disrupt interactions which stabilize the catalytically incompetent open conformation of the polymerase.

MATERIALS AND METHODS

Wild-type (wt) and mutant T7RNAPs were prepared as described previously (*20*). 3′-dNTPs were from TriLink Biotechnologies. Plasmid DNAs were purified using the Qiagen kit, per the manufacturer's instructions. Transcription reactions were carried out in 40 mM Tris, pH 7.9, 6 mM $MgCl_2$, 10 mM DTT, 10 mM NaCl, 2 mM spermidine, and 0.5% Tween-20 in 50 μL reaction volumes at room temperature with template and RNAP at 0.1 and 0.05 μM, respectively. Reactions were initiated by addition of NTPs to mixtures containing all other reaction components (preincubated for 10 min at room temperature). NTP concentrations and the labeling NTPs were as specified in individual figure legends. Reaction aliquots were removed at different times and mixed with equal volumes of stop buffer (95% formamide, 10 mM Tris, pH 8.0, 10 mM EDTA, 0.1% xylene cyanol). In some cases, RNase A was added to a final concentration of 0.1 mg/mL after the reactions had been terminated with stop buffer. The RNase A remained sufficiently active under these conditions to digest all pyrimidine-containing RNAs to completion (*21*). Separation of free transcripts from transcripts retained with elongation complexes was done as described previously (*22*, *23*). To measure rates of pyrophosphorolysis, terminated elongation complexes were formed by replacing one NTP in the transcription reaction with a 3′-dNTP. Complexes were then washed with transcription buffer in ultracentrifuge tubes to remove NTPs. The reactions were recovered, PP_i was added to 1 mM, and reaction aliquots were analyzed at different times. Analysis of the 5′-ends of transcripts made on pPK5 was done by annealing transcripts to oligonucleotides complementary to the +1 to +14 transcript sequence but containing either 0 or 2 extra C's at the 3′-end, followed by RNase T1 treatment. Transcripts were resolved by electrophoresis in TBE on 20% polyacrylamide, 1% bis-acrylamide gels containing 6 M urea. Visualization and quantification of the transcripts was done with a Molecular Dynamics Storm phosphorimager using ImageQuant software. Nonlinear least-squares fitting of these data was done with the Microcal Origin program.

RESULTS

Measurement of the Rates of Mispair Formation. Misincorporation was measured by running transcription reactions with one or more NTPs omitted so that extension beyond a defined transcript length required incorporation of a noncomplementary base. Initiation by T7RNAP requires a purine-rich initially transcribed sequence (ITS; *24*), so we used a set of templates in which the ITS contains only G's and A's. A representative experiment carried out with the template pPK10 is shown in Figure 1. The +1 to +20 sequence of the transcript from pPK10 is GGGAGAGGGAGGGAUCCCUC. When this template is transcribed in the presence of only 2 mM GTP and 0.1 mM ATP (Figure 1A, lanes 1−6) or 2 mM ATP and 0.1 mM GTP (Figure 1D, lanes 1−6), transcription halts at the first occurrence of a purine in the template strand, and a 14 base transcript is made. Over the course of an 80 min reaction, the amount of the 14mer slowly decreases while the amounts of larger transcripts (15−17mers) increase. To determine whether the 15−17mers in these reactions are made by misextension of the 14mer, or by faithful extension due to NTP contamination, we used base-specific RNases and we also took advantage of the small differences in electrophoretic migration caused by addition of different bases to a transcript. Lane 1 of Figure 1B shows the transcripts obtained after an 80 min reaction with the pPK10 template and with 2 mM GTP and 0.1 mM ATP in the reaction. Lane 2 shows the products obtained upon RNase A treatment of this reaction. The RNase treatment reveals that there is a small amount of RNase A sensitive transcript in lane 1 (indicated as '14+Y+R*') which generates the product labeled '14+Y^' in lane 2 (in these figures, misincorporated bases are indicated with an asterisk and RNase cleavage is indicated by a '^'). The bulk of the transcripts in lane 1 (>90%) are, however, RNase A resistant, and since the 16mer labeled '14+2R*' in lane 1 is RNase A resistant it must contain a misincorporated purine at +15. Upon addition of CTP and UTP (lane 3), most of the products labeled '14' and '14+G*' in lane 1 are chased to runoff transcripts. Two predominant products are obtained upon RNase A treatment of this chased reaction (lane 4). The product labeled '14+G*+C^' in lane 4 must have a misincorporated purine at +15. The '14+G*+C^' product must derive from the '14+G*' transcript indicated in lane 1 since the amount of the '14+G*+C^' product is equal to the amount of '14+G*' product which is chased upon addition of CTP and UTP. Therefore, the transcript labeled '14+G*' must have a purine misincorporated at +15. The slower electrophoretic migration of the '14+G*' product in lane 1 of Figure 1B compared to the '14+A*' product in lane 1 of Figure 1E reveals further that the misincorporated purine is a guanosine [side-by-side electrophoresis of 15mers identical in base composition from +1 to +14, but 3′-terminated with either G, A, U, or C (not shown) reveals that addition of a purine to a transcript causes a larger shift in migration than addition of a pyrimidine, and that addition of a G causes a larger shift than addition of an A]. The other predominant RNase A digestion product in lane 4 is labeled '14+Y^', and the amount of this product is equal to the sum of the amount of 14mer which is chased upon CTP/

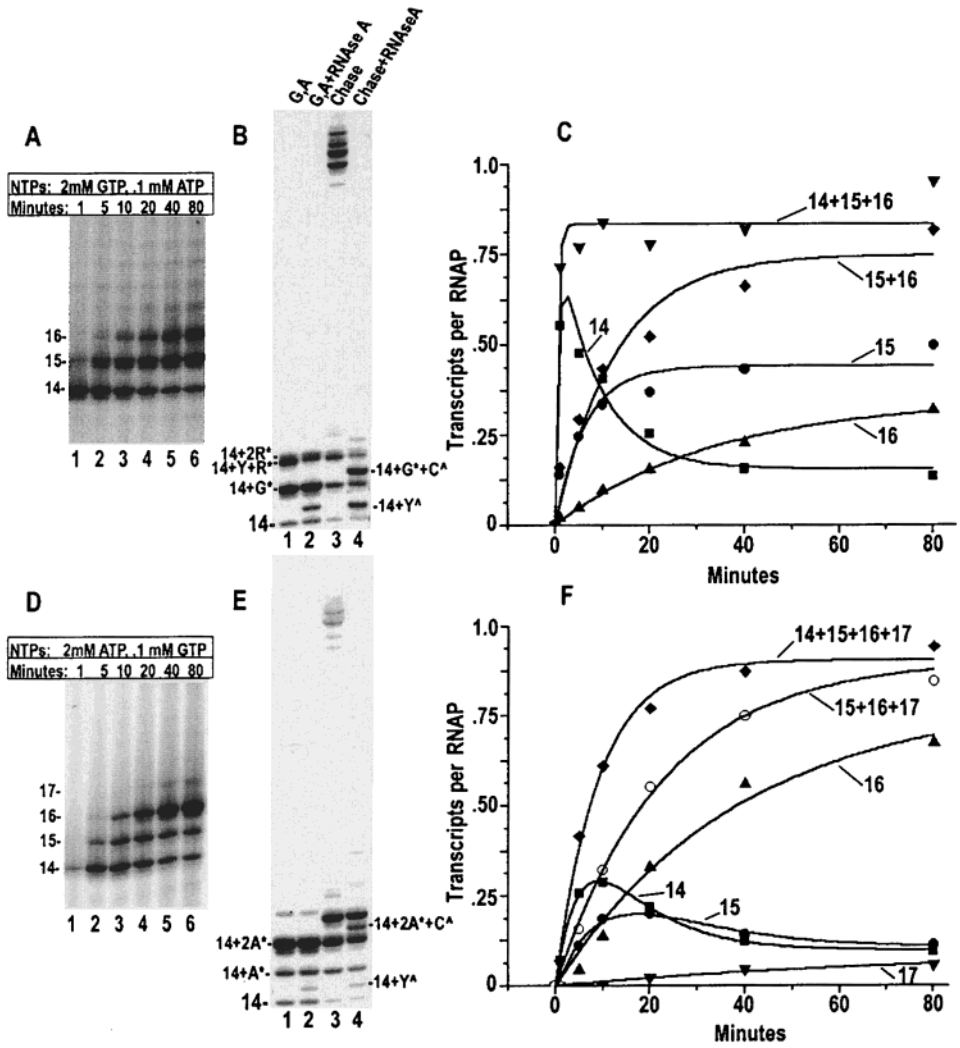

FIGURE 1: Analysis of mispair structure and misincorporation rates. (A) Transcription of pPK10 with 2 mM GTP+0.1 mM ATP. (B) Lane 1: 80 min reaction point from panel A. Lane 2: RNase A treatment of lane 1. Lane 3: UTP/CTP chase of lane 1. Lane 4: RNase A treatment of lane 3. (C) Plot of the amounts of the indicated transcripts obtained in the experiment in panel A. (D−F) As in panels A and B, but for reactions with 2 mM ATP+0.1 mM GTP.

UTP addition and the amount of the '14+Y+R*' product. From this analysis, we can conclude that most of the 15−17mers made in the reaction in Figure 1A derive from misincorporation of a G at +15. The rate of this misincorporation reaction can then be estimated as shown in Figure 1C. If we plot the total amount of transcripts ('14+15+16'mers) vs time, we see that 5 min after initiation of the reaction the total amount of transcript reaches a level equal to ~1 transcript for every RNAP molecule present and does not change significantly over the next 75 min (RNAP is the stoichiometrically limiting reagent in these reactions). The rate of production of the total transcript reflects the rate of promoter clearance and is fit to: $[\text{RNAP}](1 - e^{-k_0 t})$. The rate of 14mer production shows a rapid burst, reflecting the initial rate of 14mer synthesis (promoter clearance), and a slow decrease, reflecting the subsequent extension of the 14mer to 15- and 16mers. The rate of 14mer production is therefore fit to: $[\text{RNAP}](1 - e^{-k_1 t}) - A_2(1 - e^{k_2 t})$, where k_1 should equal the rate of promoter clearance and k_2 should equal the rate of extension of the 14mer. The rates of promoter clearance as measured from the burst phase of 14mer synthesis ($k_1 = 1.0$ min^{-1}) or the rate of total transcript production ($k_0 = 0.99$ min^{-1}) are in good agreement. The rate of extension of the 14mer as measured from the rate of 14mer decrease following completion of the burst (k_2) is 0.080 min^{-1}. Since the total amount of transcript ('14+15+16'mers) does not change significantly after the burst is complete, the increase in the amount of '15+16'mers over the course of the reaction must come at the expense of the 14mer. The rate of increase in the amount of '15+16'mers was fit to $A_2(1 - e^{-k_3 t})$ and equaled 0.079 min^{-1}, which is in good agreement with the rate of 14mer decrease. Though some extension of the 14mer is due to contamination by pyrimidine triphosphates, the fraction of transcripts which incorporate a pyrimidine at +15 is only ~10% of total (i.e., the '14+Y' product in lane 2, Figure 1B), so that the rate of 14mer *mis*extension due to incorporation of a G at +15 is closely approximated by the rate of 14mer extension (Table 1).

Panels D−F of Figure 1 present a similar analysis except that A, rather than G, misincorporation at +15 was forced by using high ATP (2 mM) and low GTP (0.1 mM) concentrations in the reaction. The differences in electrophoretic migration seen when different misincorporation reactions were run side-by-side (not shown) confirmed that G misincorporation predominated when a high GTP/low ATP concentration was used and vice versa. A significant differ-

Table 1: Rates of Mispair Formation

mispair formed	template/position/[NTP][a]	rate (min^{-1})
rA**rG** dT**dG**dA	pPK5/+15/2 mM	0.0030−0.0040
rA**rG** dT**dG**dA	pPK7/+23/2 mM	0.0051−0.0069
rG**rG** dC**dG**dG	pPK13/+20/2 mM	0.029−0.031
rA**rA** dT**dG**dA	pPK5/+15/2 mM	0.0040−0.0045
rA**rA** dT**dG**dA	pPK7/+23/2 mM	0.0076
rG**rA** dC**dG**dG	pPK13/+20/2 mM	0.011−0.015
rA**rG** dT**dA**dG	pPK10/+15/2 mM	0.075−0.079
rA**rG** dT**dA**dC	pPK13/+15/2 mM	0.25
rA**rA** dT**dA**dG	pPK10/+15/2 mM	0.070−0.080
rA**rA** dT**dA**dC	pPK13/+15/2 mM	0.13−0.19
dArC**rC** dTdG**dA**	pPK5/+16/0.5 mM	0.67
rA**rC** dT**dA**dG	pPK10/+15/0.5 mM	0.14
rA**rU** dT**dG**dA	pPK5/+15/0.5 mM	0.27
rArU**rU** dTdA**dG**	pPK10/+16/0.5 mM	1.1

[a] The template used, the position of the mispair (relative to the +1 start site), and the concentration of the NTP used in the misincorporation step are given. All the templates contain a promoter identical in sequence to the T7 promoter consensus from −17 to +5. Starting at +6, the relevant transcript sequences are the following: pPK5, GGAGGGAGACUGCAG; pPK7, GGAGGGAGGGAGGGAGACU; pPK10, AGGGAGGGAUCCCUC; pPK13, AGGGAGGGAUGGAGC.

ence in reaction kinetics at high vs low GTP concentrations was seen in that promoter clearance was slower at the lower GTP concentrations. This is obvious from inspection of Figure 1D,F, where it is seen that the total amount of transcripts ('14+15+16+17'mers) does not reach a plateau until ∼20 min after initiation of the reaction and where the rate of clearance fits to 0.11 min^{-1} as assessed from the rate of total transcript production, or 0.16 min^{-1} as assessed from the burst phase of 14mer production. As will be shown later (Figure 6), this slower rate is also seen on another template (pPK5), where it is due to a pause that ocurs during clearance when the RNA reaches 6 bases in length. The rate of A misincorporation at +15 on pPK10 as determined from the data shown in Figure 1D−F was 0.07−0.08 min^{-1} (Table 1). Using analyses similar to those detailed above, rates for 14 misincorporation reactions were measured. All of these data are summarized in Table 1.

RNAs Containing Mispairs Near Their 3′-Ends Are Extended More Slowly than Correctly Paired Termini. To determine whether mispairs are extended more slowly than correctly paired termini, we ran reactions using either pPK10 or pPK5 as templates and containing only 2 mM GTP and 0.1 mM ATP or 2 mM ATP and 0.1 mM GTP (the +1 to +20 transcript sequence of pPK5 is GGGAGGGAGG-GAGACUGCAG). After 80 min to allow formation of mispaired RNAs, the reactions were chased with either high (0.5 mM) or low (0.05 mM) concentrations of CTP and UTP, and reaction time points were taken between 10 s and 20 min. A representative experiment which used pPK10 as the template and high ATP/low GTP concentrations in the misincorporation reaction is presented in Figure 2. It is apparent from panel A of this figure that RNAs bearing 3′-mispairs are extended more slowly than RNAs with correctly paired termini. For example, even at the low CTP/UTP concentrations (Figure 2A, lanes 9−16), ∼70% of the 14mer is chased to full-length transcripts within 10 s of initiation of the chase (the remaining ∼30% of the 14mer is not chased at all). However, the 15mer, which bears a single mispair at its 3′-end, is chased much more slowly, and the 16mer (which has two 3′-mispairs) is barely chased at all. At higher CTP/UTP concentrations (lanes 1−8), the chaseable fraction of the 15mer is extended rapidly (though ∼60% of the 15mer cannot be chased at all), and extension of the 16mer is also seen. However, very little of the 16mer is chased to runoff product. Instead, two intermediates (labeled 17′ and 18) accumulate. Presumably the 17′mer and 18mer contain, respectively, one and two correctly paired bases at their 3′-ends, yet these intermediates are chased to longer RNAs even more slowly than the doubly mispaired 16mer (otherwise they would not accumulate to the extent that they do). This shows that mispairs one or two base pairs away from the RNA 3′-end can severely hinder extension, even when the 3′-end itself is correctly paired.

The amounts of the different transcripts for the experiment shown in Figure 2A are plotted vs time in Figure 2B, C. Because heparin was added simultaneously with initiation of the chase in these reactions, initiation of new transcription was suppressed, and the total molar amount of transcripts remained constant over the course of the reaction. This allowed product−precursor relationships to be defined based on the agreement between the rates and amplitudes of disappearance of certain transcripts and the appearance of others (for example, the 17′mer and 18mer if Figure 2A must derive from the 16mer since they only appear as the 16mer disappears). Rates for extension of correctly paired RNAs and for different mispairs were then determined by fitting the data as shown in Figure 2B, C, and as described in the legend to Figure 2. Mispair extension rates were similarly determined for pPK10 at high GTP/low ATP concentrations, and for pPK5 at high GTP/low ATP concentrations and at high ATP/low GTP concentrations. All of these data are summarized in Table 2.

RNAs That Cannot Be Chased Are Associated with 'Dead-End Complexes'. It is apparent from Figure 2 that a significant fraction of the transcripts present in the misincorporation reaction cannot be chased at all upon addition of CTP and UTP. For example, while ∼70% of the 14mer and ∼40% of the 15mer are chased to longer products within 20 s of addition of 0.5 mM CTP and UTP in lanes 1−8 of Figure 2A, the remaining fraction of 14mer and 15mer is not extended over the next 20 min. The presence of unchaseable transcripts could be due to a fraction of the halted complexes dissociating, since transcripts released into solution would not be substrates for extension, or it could be due to the complexes collapsing into 'dead-end' states, which retain but can no longer extend the RNA. To distinguish these possibilities, we filtered reactions to separate released transcripts from those still associated with transcription complexes. When a misincorporation reaction was subjected to ultrafiltration, the transcripts were found almost exclusively in the retenate (Figure 2D, lane 2) and not in

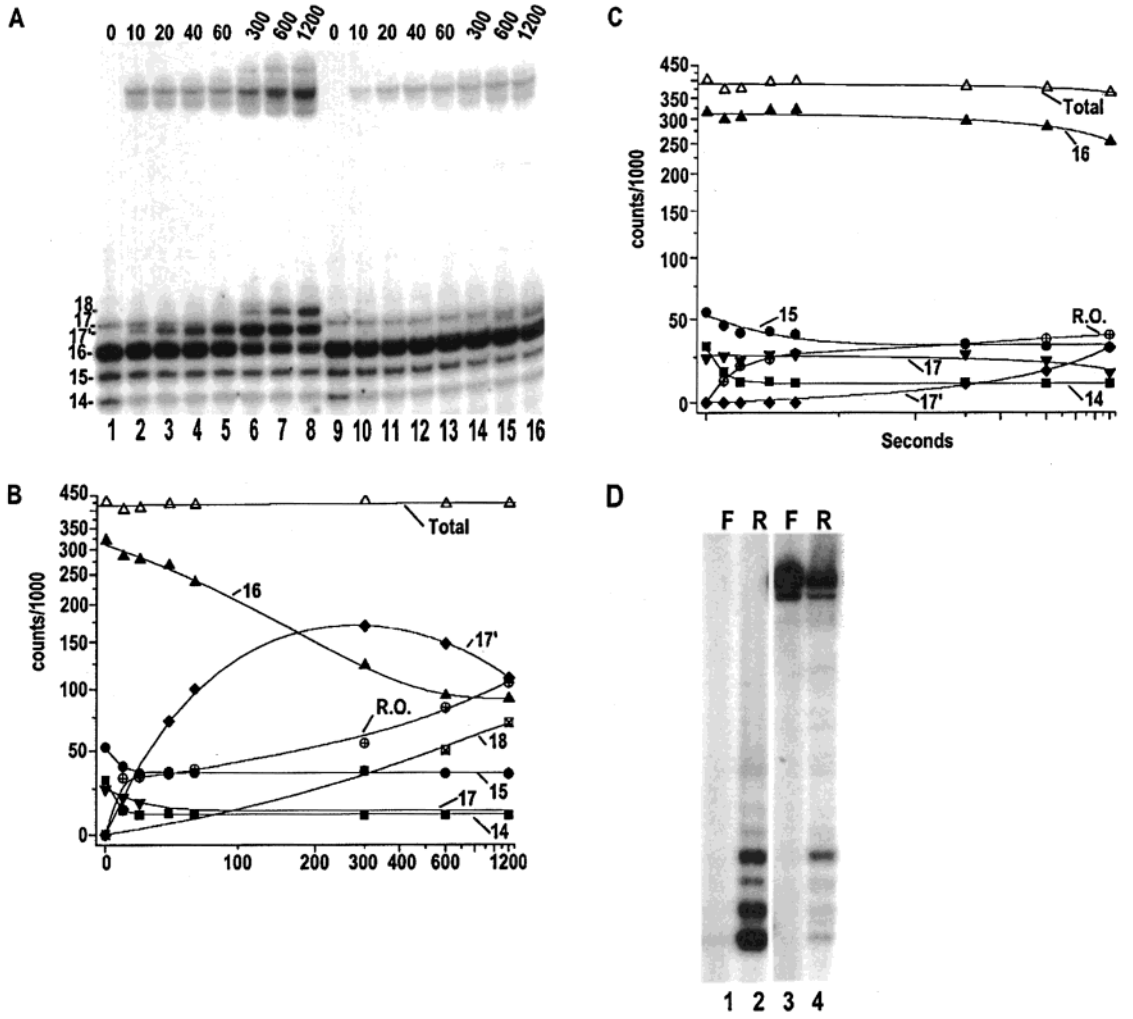

FIGURE 2: Measurement of the rates of mispair extension. (A) Lanes 1, 9: transcripts obtained after an 80 min transcription reaction using pPK10 as template and 2 mM ATP+0.1 mM GTP. Lanes 2−8 and 10−16: chase of the reactions in lanes 1 and 9, with, respectively, 0.5 and 0.05 mM CTP+UTP. (B) Plot of the amount of each transcript vs time for lanes 1−8 of panel A. Open triangles, total transcription; filled squares, 14mer; filled circles, 15mer; filled triangles, 16mer; inverted filled triangles, 17mer; filled diamonds, 17′mer; squares with crosses, 18mer; circles with crosses, runoff transcripts. Rates of disappearance of the 14-, 15-, 16-, and 17mers were fit to $Y_0 + Ae^{-kt}$. The change in the 17′- and 18mer was fit to $A_1(1 - e^{-k_1 t}) - A_2(1 - e^{-k_2 t})$ where A_1 and k_1 were equal to the rate and amplitude of disappearance of the precursor 16mers or 17′-mers, respectively. Runoff transcription was fit to $A_1(1 - e^{-k_1 t}) + A_2(1 - e^{-k_2 t})$, corresponding to a burst of synthesis due to rapid extension of the 14- and 15mers, followed by a slower accumulation due to extension of the 17′- and 18mers. (C) As in (B), but for lanes 9−16 of panel A. (D) Ultrafiltration through 100 kDa MW cutoff membranes of reactions run for 80 min with pPK5 with 0.5 mM GTP and 0.5 mM ATP. Lane 1, filtrate; lane 2, retenate; lane 3, filtrate of the UTP+CTP chase of the misincorporation reaction; lane 4, retenate of the chased reaction.

the filtrate (lane 1). When this misincorporation reaction was first chased and then filtered, most of the runoff transcript was found in the filtrate (lane 3), but all of the transcripts that were not chased remained in the retenate. Similar results were obtained with the other templates (not shown), indicating that transcripts that fail to chase have not been released but are instead associated with 'dead-end' complexes.

T7RNAP Does Not Display Nucleolytic Proofreading. T7RNAP has been reported to have RNA cleavage activity (*19*), but even in 80 min incubations we never detected any cleavage products in these misincorporation assays. Since it is possible that in these reactions transcripts were being continuously cleaved and re-extended, we carried out reactions in which chain-terminated transcripts were generated on pPK5 by including either 3′-dCTP or 3′-dUTP along with GTP and ATP in the reaction (Figure 3). Subsequently, CTP and UTP in 10-fold excess of the 3′-dNTP were added to these reactions along with heparin to limit reinitiation. Since the transcripts in these halted complexes lack a 3′-OH, they cannot be extended. However, if a 3′-OH group is generated by cleavage, the transcripts will be subsequently extended because the CTP and UTP are in 10-fold excess of the 3′-dNTP. Lane 1 of Figure 3 reveals that a predominant 15mer is formed by incorporation of 3′-dCMP during transcription of pPK5 in the presence GTP, ATP, and 3′-dCTP. One (lane 2) or twenty (lane 3) minutes after addition of CTP and UTP to this reaction, little or none of this 15mer has been extended to longer transcripts. In lane 4, the reaction included 3′-dUTP instead of 3′-dCTP. Because misincorporation of 3′-dUMP is slower than incorporation of 3′-dCMP, some 14mer remains in this reaction. One minute after addition of CTP and UTP (lane 5), all of this 14mer has been extended, confirming that transcripts bearing a 3′-OH group are extended upon addition of CTP and UTP. However, the 3′-dUMP-terminated 15mer is not extended even after 20 min (lane 6). Together with our failure to observe the accumula-

Table 2: Rates of Faithful Extension of Misincorporation Products

Extension Reaction	[NTP]*	Rate
rA rArU dTdA → dTdA	.005 mM	6.8 min^{-1}
rA rArU dTdA → dTdA	.5 mM	>20 min^{-1}
rA**rA** rA**rA**rC dT**d**AdG → dT**d**AdG	.005 mM	1.5 min^{-1}
rA**rA**rA rA**rA**r**A**rC dT**dAdG**dG → dT**dAdG**dG	.005 mM	.015 min^{-1}
rA**rA** rA**rA**rC dT**d**AdG → dT**d**AdG	.5 mM	9.2 min^{-1}
rA**rA**rA rA**rA**r**A**rC dT**dAdG**dG → dT**dAdG**dG	.5 mM	.39 min^{-1}
rA**rA**r**A**rC rA**rA**r**A**rCrC dT**dAdG**dGdG → dT**dAdG**dGdG	.5 mM	.08 min^{-1}
rA**rG** rA**rG**rC dT**d**AdG → dT**d**AdG	.005 mM	.33 min^{-1}
rA**rG** rA**rG**rC dT**d**AdG → dT**d**AdG	.5 mM	19 min^{-1}
rA**rG**rC rA**rG**rCrC dT**d**AdGdG → dT**d**AdGdG	.005 mM	.04 min^{-1}
rA**rG**rC rA**rG**rCrC dT**d**AdGdG → dT**d**AdGdG	.5 mM	1.3 min^{-1}
rA rArC dTdG → dTdG	.005 mM	11 min^{-1}
rA rArC dTdG → dTdG	.5 mM	>20 min^{-1}
rA**rA** rA**rA**rU dT**dG**dA → dT**dG**dA	.005 mM	n.d.
rA**rA** rA**rA**rU dT**dG**dA → dT**dG**dA	.5 mM	.71 min^{-1}
rA**rA**rU rA**rA**rUrG dT**dG**dAdC → dT**dG**dAdC	.1 mM	.033 min^{-1}
rArCrUrG rArCrUrGrC dTdGdAdCdG → dTdGdAdCdG	.005 mM	1.2 min^{-1}
rA**rG** rA**rG**rU dT**dG**dA → dT**dG**dA	.005 mM	n.d.
rA**rG** rA**rG**rU dT**dG**dA → dT**dG**dA	.5 mM	.65 min^{-1}

[a] Concentration of the NTP used in the specified extension reaction. Rates were determined from experiments such as those shown in Figure 2. nd indicates that there was no detectable extension for the specified reaction and NTP concentration. In cases where extension was too fast too measure manually, the rate is given as >20 min^{-1}. Mispairs are in boldface type.

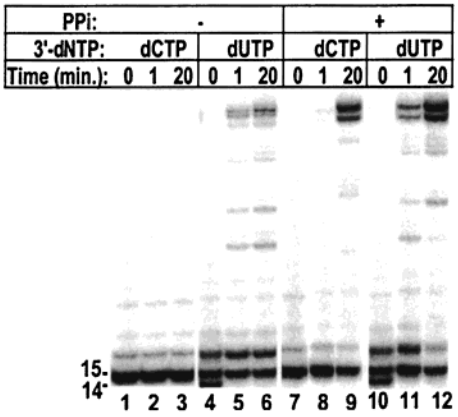

FIGURE 3: Transcripts in halted ECs are not cleaved, but are sensitive to pyrophosphorolyis. Elongation complexes containing chain-terminated 15mers formed by incubating pPK5 with RNAP, 0.5 mM GTP, 0.5 mM ATP, and either 0.1 mM 3′-dCTP (lanes 1, 7) or 3′-dUTP (lanes 4, 10) were chased for 1 (lanes 2, 5, 8, 11) or 20 (lanes 3, 6, 9, 12) min with 1 mM CTP and UTP, either with (lanes 7−12) or without (lanes 1−6) 1 mM PP_i.

tion of cleavage products in the misincorporation assays, these results indicate that T7RNAP cannot cleave transcripts in elongation complexes, or that it does so very slowly. This implies that T7RNAP lacks any endogenous proofreading ability, and this conclusion is supported by the observation that the amount of purine misincorporation, as assessed by RNase A digestion of chased misincorporation reactions, is similar to that seen before the reactions are chased (as can be seen in Figure 1B,E), indicating that the misincorporated purines are not removed before the transcripts are extended.

We did find, however, that 3′-dNMP-terminated transcripts *could* be extended if the 3′-base was first removed by pyrophosphorolysis in reactions in which 1 mM PP_i was added during the chase (Figure 3; lanes 7−12). Processive pyrophosphorolysis was also seen in elongation complexes to which PP_i was added after NTPs were removed by ultrafiltration (not shown). Since mispairs are extended more slowly than correctly paired RNAs, this raises the possibility that pyrophosphorolysis could contribute to proofreading, especially if the presence of a mispair reduced the rate of pyrophosphorolysis less than the rate of forward extension. We tested this by chasing misincorporation products in the presence or absence of 1 mM PP_i to see if pyrophosphorolysis would remove misincorporated bases from the transcripts before they were extended, but we found that the presence of mispairs in the chased transcripts was not reduced by including PP_i in the chase reaction (data not shown). This indicates that pyrophosphorolysis does not remove misincorporated bases before the misincorporation products are extended, and suggests further that both pyrophosphorolysis and forward extension are similarly slowed by the presence of a mispair.

Misincorporation Properties of T7RNAP Mutants. A total of 45 different T7RNAP mutants at 31 different positions were tested for effects on misincorporation (the legend to Figure 6A lists the mutants tested). Only four mutations (G640A, F644A, G645A, H784A) were found to increase misincorporation rates in reactions which used pPK5 as template (Figure 4). Mutants F644A, G645A, and G640A misincorporated AMP 7−9-fold faster than the wt enzyme (Table 3). H784A increased this misincorporation rate by

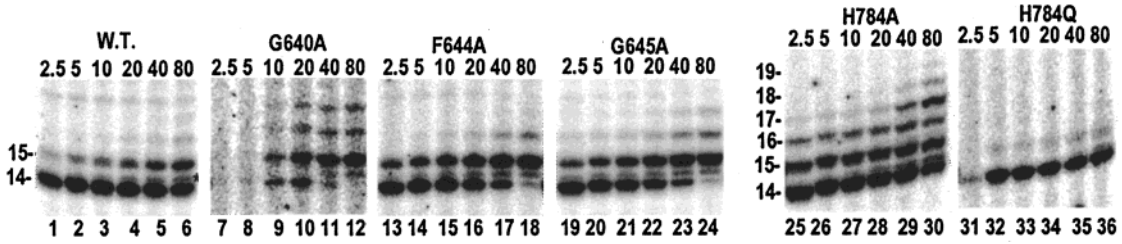

FIGURE 4: Mutants which show increased rates of mispair formation or mispair extension. Reactions were run with pPK5, 0.1 mM GTP, 2 mM ATP, and the indicated RNAPs for the times indicated (in minutes). The delayed appearance of the 14mer in the reaction with G640A reflects a slower catalytic rate for this mutant. To distinguish misincorporation from extension due to the presence of contaminating pyrimidine triphosphates, the reactions were treated with RNase A. The minor transcript indicated with an asterisk in lane 6 is produced by RNase A digestion and reveals the presence of a small amount of contaminating pyrimidine triphosphate in the reactions.

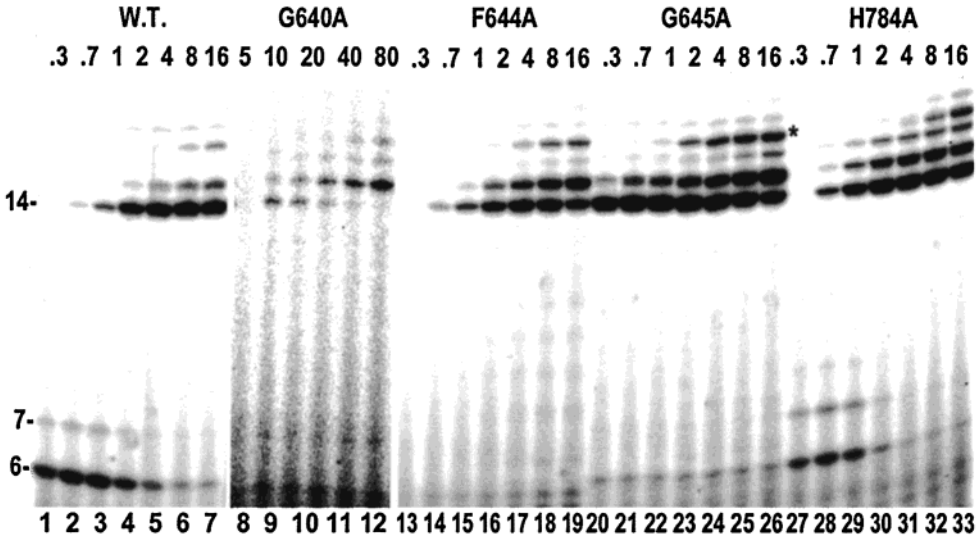

FIGURE 5: Effects of T7RNAP mutations on pausing during promoter clearance. Reactions were run as in Figure 4 for the times indicated (in minutes). Pausing at +6 (and to a lesser degree at +7) is apparent in the wt and H784A reactions, but not in the reactions with the other three enzymes (unlike the reactions in Figure 4, these reactions were not RNase A treated; the transcript indicated with an asterisk in lane 26 is RNase A sensitive).

Table 3: Misextension Rate, Promoter Escape, and +6 Pause Lifetimes of wt and Mutant T7RNAPs[a]

RNAP	misextension rate[b]	promoter escape	half-life of +6 pause
wt	0.006 min^{-1}	0.29 min^{-1}	2.2 min
F644A	0.042 min^{-1}	0.40 min^{-1}	nd
G645A	0.056 min^{-1}	2.0 min^{-1}	nd
G640A	0.059 min^{-1}	0.14 min^{-1}	nd
H784A	0.017 min^{-1}	0.50 min^{-1}	1.3 min

[a] Reactions contained pPK5 as template, GTP and ATP at 0.1 and 2 mM, respectively, and no CTP or UTP; nd = not detectable. [b] The misextension reaction was misincorporation of rA opposite dG at +15 on pPK5.

only 2−3-fold. However, the H784A mutant also enhanced mismatch extension and generated a ladder of RNase A resistant transcripts extending up to 19 bases in length (Figure 4, lanes 25−30). In contrast, with the G640A, F644A, and G645A mutants, the predominant misextension product was a 15mer. Thus, the H784A mutation increased both misextension and mismatch extension, while the G640A, F644A, and G645A mutations enhanced misextension but not mismatch extension. It is also apparent that an H784Q mutation did not increase misextension (Figure 4, lanes 31−36).

The G640A, F644A, and G645A Mutations Eliminate Pausing at +6. As noted previously, promoter clearance on pPK5 and pPK10 by the wt enzyme is slow at low GTP concentrations. As shown in lanes 1−7 of Figure 5, on pPK5 this is due to pausing during promoter clearance, particularly at the point when the RNA reach 6 bases in length. Figure 5 also shows that this pause is not seen with the G640A, F644A, and G645A mutants (lanes 8−26). Because of the generally reduced extension rates of the F644A and G640A mutations, the elimination of the +6 pause does not increase the rate of promoter clearance of these mutants; however, the G645A mutant does clear the promoter ~7-fold faster than the wt enzyme (lanes 20−26 and Table 3). The H784A mutant is again seen to be distinct from the G640A, F644A, and G645A mutants in that it continues to pause at +6.

DISCUSSION

Context, Position, and Base Effects on Misincorporation. At two different template positions but in identical sequence contexts (pPK5, +15; pPK7, +23), the rates of T7RNAP misincorporation of either A or G opposite dG are similar and range from 0.0035 to 0.0076 min^{-1}. In a different sequence context (pPK13, +20), purine misincorporation opposite dG is 4−5-fold faster (Table 1). It is possible that this context effect reflects the identity of the 3′ base-pair. At +20 on pPK13, this is an rG·dC pair, while at the points of misincorporation on the other two templates it is an rA·dT pair. T7RNAP preferentially initiates with GTP, and the X-ray structure of a T7RNAP transcription complex (*7*)

suggests that H784 makes a base-specific hydrogen bond with the N3 of the transcript 3′-rG. Such interactions could enhance both faithful extension and misextension of base-pairs in which the 3′ RNA base is a G. We also found that purine misincorporation opposite dA is 10−20-fold faster than opposite dG, and that misincorporation of pyrimidines opposite template purines occurs more readily than purine misincorporation. In identical sequence contexts, misincorporation of rC or rU opposite dA or dG is, respectively, 2- or 70-fold faster than purine misincorporation, even when the pyrimidine triphosphate concentration is one-fourth the purine triphosphate concentration (Table 1). The preferential misincorporation of pyrimidines opposite purines is also evident from the fact that pyrimidine misincorporation predominates in reactions where GTP, ATP, and either UTP or CTP are present at similar concentrations. For example, in the reaction shown in lanes 4 and 10 of Figure 2A, GTP, ATP, and 3′-dUTP are all present, but it is predominantly 3′-dUTP which is misincorporated and leads to formation of the chain-terminated 15mer. Similar observations were made with *E. coli* RNAP, where it was seen that in the presence of UTP, GTP, and ATP it was predominantly UMP which was misincorporated opposite dGMP (*2*).

T7RNAP Fidelity Depends on Stringency during Incorporation and Not on Postincorporation Proofreading. Reports of RNase activity in T7RNAP preparations (*19*) raise the possibility that T7RNAP has a transcript cleavage activity which could contribute to proofreading. The experiments shown in Figure 3, in which transcripts are first chain-terminated with 3′-dYMPs and then chased with excess YTPs, should be very sensitive to the presence of transcript cleavage in the elongation complex but failed to reveal such activity, though pyrophosphorolysis was readily detected upon addition of pyrophosphate. We also failed to observe any accumulation of apparent transcript cleavage products in the many experiments we have run. We cannot account for the discrepancy between our results and those reported previously by Sastry et al. (*19*), but McAllister and co-workers have also failed to detect any RNase activity in their T7RNAP preparation (*27*). If T7RNAP lacks an intrinsic proofreading activity and if pyrophosphorolysis also makes little or no contribution to proofreading, then its fidelity must be strictly dependent on stringent selection against misincorporation. An estimate of the fidelity of this enzyme may then be made by comparing the misincorporation rates measured here (Table 1) to the normal transcript extension rate of T7RNAP which, at room temperature, has been found to be ∼60 bases/s (*28*). This implies an error frequency between 1 in 10^6 and 1 in 3×10^3, depending on the mispair, with an average error frequency of 1 in 2×10^4 for the 6 mispairs examined here. This is in good agreement with an average base substitution error rate of 1 in 3.5×10^4 for T7RNAP as measured by Remington et al. (*29*), and is similar to the base substitution error rate of exonuclease-deficient DNAP I (*30*).

The GreA/B transcript cleavage activity of *E. coli* RNAP has been suggested to be important not only in proofreading but also in rescuing the elongation complex from inactivated or 'dead-end' states (*17*). Certain template sequences (*31*) and misincorporation (*2*) both promote the formation of inactivated complexes with *E. coli* RNAP. Similarly, we found that, upon prolonged incubation, halted T7RNAP elongation complexes tend to collapse into 'dead-end' states from which transcript extension either is slow or does not occur. The tendency to form such complexes is greater for complexes in which the transcript carries 3′-mismatches. Even when they do not completely arrest transcription, such mismatches can slow extension severely (Table 2). The absence of any intrinsic cleavage activity in T7RNAP which could facilitate escape from inactive or poorly active states suggests either that collapse into such states occurs rarely in vivo, or that there are as yet unidentified factors which play a role similar to GreA/B during T7RNAP transcription.

Mutations Which Do Not Increase Misincorporation Rates. We tested 45 different T7RNAP mutations for effects on misincorporation rates. Increased misincorporation rates were seen with only a small number of mutants. Minnick et al. (*30*) examined 28 DNAP I point mutants and identified only 5 positions where mutations affected fidelity. Their conclusion was that only a limited number of side chains contribute to fidelity in DNAP I. While our observations are in agreement with this, we must qualify our conclusions because we examined misincorporation rates and not fidelity. It is possible that some of the mutations which did not show increased misincorporation rates have effects on fidelity because they decrease the rates of faithful incorporation. For example, if a mutation decreases faithful incorporation rates by10-fold, but decreases misincorporation rates by only 2-fold, then it would have an effect on fidelity but would not be identified in our assay as having an increased misincorporation rate. Since many of the mutations in the palm and fingers subdomains have been previously shown to have reduced bond formation rates (*20*, *32*), we cannot rule out that some of these mutations affect fidelity.

However, the mutations K472A, P508A, L512A, E517A, R551S, D552S, L637A, Y639F, Q649S, D879E, A881T, F882Y, and ΔA883, and alanine substitutions of residues 388−395 of the thumb subdomain do not reduce elongation rates at normal NTP concentrations (refs *20*, *32*−*34*, and unpublished observations) and also do not show increased rates of misincorporation, indicating that these side chains are not important for fidelity. Inspection of a T7RNAP transcription complex structure (Figure 6A) reveals that, with the exception of Y639, these side chains do not directly contact the NTP, template, or RNA in the immediate vicinity of the active site, though the structures of a T7 RNAP transcription complex and a T7DNAP·primer-template complex imply that thumb subdomain side chains 390−395 contact the RNA 4−6 bases away from the 3′-end (Figure 6A). Apparently, disruption of these thumb−RNA interactions does not affect misincorporation. Similar observations have been made for mutations in the thumbs of RT and DNAP I, where it was shown that thumb subdomain mutations affect frameshift fidelity, but not base substitution (*35*, *36*). Tyrosine 639 stacks on the template base opposite the 3′-base of the RNA (Figure 6A), and a similar interaction between the template base and the corresponding tyrosine is seen in the open complex structures of Klentaq and *B. thermophilus* DNAPs (*10*, *11*). Mutations of this tyrosine (including a Y to F substitution) decrease fidelity in DNAP I (*30*), but we found that a Y639F mutation in T7RNAP has no effect on misincorporation rates. Other substitutions tested (Y639T, -H, or -L) also did not increase misincorporation rates, but since these substitutions have significant effects

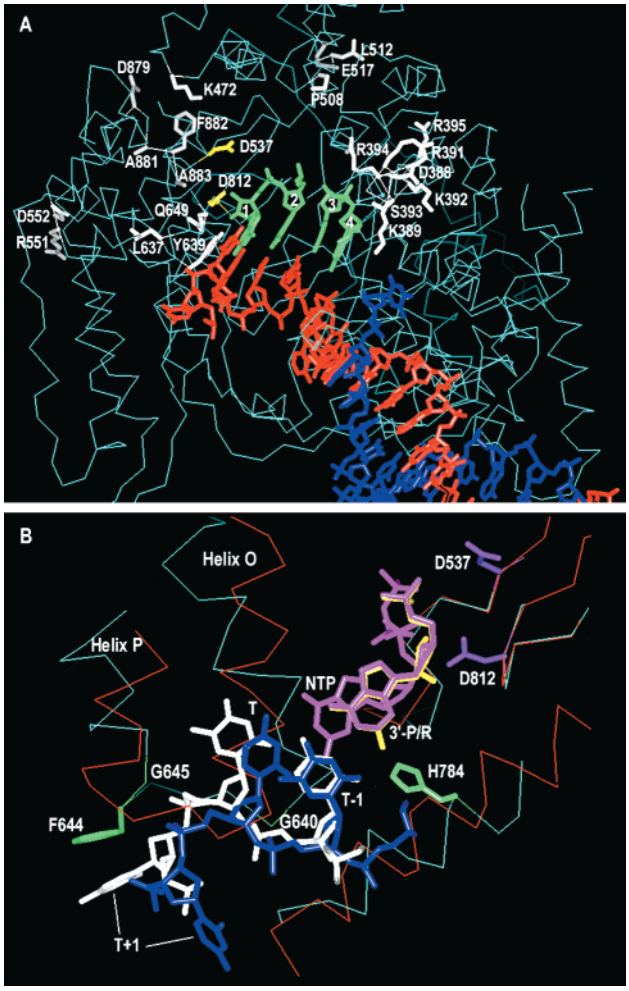

FIGURE 6: (A) The structure of a T7RNAP transcription complex (*7*) is shown with the template strand in red, the nontemplate strand in blue, and the RNA in green. This structure contains coordinates for a 2 base RNA (labeled "1" and "2"); a 2 base extension of this RNA (labeled "3" and "4") is modeled from the primer of a T7DNAP complex (*12*). The side chains of amino acids which, when mutated, neither decrease polymerase activity nor increase misincorporation rates are shown in white. The mutations tested for increased misincorporation rates were D388A, D389A, R391A, K392A, S393A, R394A, R395A, R425A, K472A, W502A, P508A, L512A, E517A, R551S, D552S, R627S, M635A, M635F, M635Y, L637A, Y639F, Y639S, Y639T, Y639H, Y639L, Y639A, G640A, S641A, F644A, G645A, Q649S, H784A, H784Q, I810S, H811A, H811S, D812A, D812E, D812S, D812N, D879E, D879E/ΔA883, D879E/A881T/ΔA883, D879E/F882W, and D879E/F882Y. (B) The active site structures of T7RNAP (in cyan) and T7DNAP (in red) were superimposed by maximizing the alignment of the main-chain atoms of D537 and D812 of T7RNAP with, respectively, D475 and D645 of T7DNAP. The side chains of D537 and D812 are in purple. The finger subdomain helices corresponding to helices O and P of DNAP I are labeled. The template strands from the T7RNAP transcription complex and T7DNAP replication complex structures are in white and blue, respectively. The 3′-base of the RNA from the T7RNAP structure is in yellow, and the 3′-base of the primer and ddNTP from the T7DNAP replication complex structure is in magenta. The main and side chains of residues which increase misincorporation when mutated (G640, F644, G645, H784) are in green. The 3′-base of the primer and RNA is labeled '3′−P/R'. The templating base and the bases immediately 5′ and 3′ to the templating base are labeled 'T', 'T+1', and 'T−1', respectively.

on polymerase activity, we draw no conclusion regarding their fidelity.

Mutations Which Increase Misincorporation. The mutations which clearly increase misincorporation rates (G640A, G644A, F645A, and H784A) are all located on the fingers subdomain in a region involved in template strand contacts. The effects of the F644A, G645A, and G640A mutations are similar, and distinct from those of the H784A mutation. We discuss first a possible mechanism for the F645A, G644A, and G640A mutations. Figure 6B shows the active site structure of a T7RNAP transcription complex. Superimposed on this structure are the template strand, 3′-primer base, and ddNTP from a T7DNAP·primer-template structure (*12*) (superposition was done by aligning the main-chain atoms of the conserved catalytic carboxylates of the two enzymes). It can be seen that the 3′ base of the primer from the T7DNAP structure and the 3′ base of the RNA from the T7RNAP structure superimpose very well, as do the template bases (T−1) opposite the primer/RNA 3′ base (3′-P/R). However, the templating bases opposite the ddNTP (T) and the template bases immediately downstream (T+1) are in different conformations in these two structures. In addition, the helices corresponding to DNAP I helices O and P are in different conformations in the two enzymes. The T7DNAP·P-T·ddNTP complex is believed to represent a catalytically competent, closed conformation. The T7RNAP transcription complex structure almost certainly represents a catalytically incompetent open complex for the following reasons: (1) It lacks NTP, and both the kinetic and structural data indicate that isomerization to the closed complex is driven by NTP binding (*9*−*13*). (2) The position and conformation of the templating base, the fingers subdomain, and the conserved Y639 side chain are similar to those seen in the open complex structures of Klentaq and *B. thermophilus* DNAPs (*10*, *11*). Inspection of Figure 6B therefore immediately suggests a mechanism for the F644A mutation, since the isomerization of the transcription complex from an open to a closed form would involve movements of the fingers subdomain and template strand which would probably disrupt the stacking interaction between F644 and the T+1 template base. We therefore propose that the interaction between F644 and the T+1 template base represents *an inhibitory ground state interaction which specifically stabilizes the catalytically incompetent open conformation*. The G640A and G645A mutations may also increase misincorporation by disrupting interactions between the template and RNAP in the open conformation. The G645 C-α is only 2.59 Å from the phosphate oxygen of the T base. A larger side chain would prevent the close approach of the template strand and could disrupt the interaction of the T+1 base with the adjacent F644 side chain. G640 occurs in a turn at the end of helix O where a larger side chain cannot be accommodated without disrupting the structure of the loop connecting helices O and P which binds the template strand in the open complex (Figure 6B).

It has been proposed that polymerase mutations which increase misincorporation facilitate accommodation of incorrect base pairs in the catalytically competent closed conformation of the active site or in the transition state (*30*, *37*). However, the widely accepted induced fit mechanism for polymerase fidelity allows, at least theoretically, for the possibility that interactions which limit misincorporation may also function by stabilizing the catalytically incompetent open state. Our observations suggest that such interactions exist, and that the F644A, G645A, and G640A mutations increase misincorporation by disrupting such interactions. Additional

evidence for this comes from the observation that the F644A, G645A, and G640A mutations eliminate the pause at +6 which is observed with the wt enzyme on the pPK5 promoter. The possibility that fidelity requirements may limit the speed of DNA or RNA synthesis has been suggested, and interactions which stabilize catalytically incompetent states of the polymerase could obviously have such effects. The G640A, F644A, and G645A mutations do not generally increase transcript extension rates (*32*), but these substitutions may also slow catalysis in the closed complex so that, even if they enhance the open to closed isomerization by destabilizing the open state, they may cause no *net* increase in extension rate. However, transcript extension rates are known to vary enormously as a function of sequence (*38*), and it is easy to imagine that many positions at which transcription is slowed or the apparent K_{NTP} is increased reflect points at which the balance between catalytically competent and incompetent states of the polymerase is tilted heavily toward the incompetent state. We suggest that T7RNAP pauses at +6 on the pPK5 promoter for this reason. At such pauses, mutations which destabilize the catalytically incompetent state might enhance extension rates. This may explain why the G640A, F644A, and G645A mutations eliminate the +6 pause.

While the G640A, F644A, and G645A mutations increase misincorporation rates, they do not appear to enhance mismatch extension. In contrast, the H784A mutant exhibits a slower rate of misincorporation, but is better at extending mismatches (Figure 4). The distinct effect of the H784A mutation on mismatch extension is interpretable in terms of the structure of a transcription complex. Figure 6B shows that the H784 side chain interacts with the 3′ RNA·template base pair. Loss of the H784 side chain may therefore facilitate accommodation of a 3′ mispair in the active site. H784 may hydrogen bond either to the N2 of a guanosine at the RNA 3′-end and/or to the O2 of a template pyrimidine at T−1. We reasoned that a glutamine side chain should be able to make a similar set of interactions and would therefore not affect misincorporation or mismatch extension. This expectation was confirmed by the properties of an H784Q mutation (Figure 4).

ACKNOWLEDGMENT

We thank Pamela Karasavas and William T. McAllister for providing the pPK series of plasmids (*39*) used in these studies.

REFERENCES

1. Kirkwood, T. B. L., Rosenberger, R. F., and Galas, D. J., Eds. (1986) *Accuracy in Molecular Processes*, Chapman and Hall, London.
2. Erie, D. A., Hajiseyedjavadi, O., Young, M. C., and von Hippel, P. H. (1993) *Science 262*, 867−873.
3. Thomas, M. J., Platas, A. A., and Hawley, D. K. (1998) *Cell 93*, 627−637.
4. McAllister, W. T., and Raskin, C. A. (1993) *Mol. Microbiol. 10*, 1−6.
5. Sousa, R., Chung, Y. J., Rose, J. P., and Wang, B. C. (1993) *Nature 364*, 593−599.
6. Cheetham, G. M., Jeruzalmi, D., and Steitz, T. A. (1999) *Nature 399*, 80−83.
7. Cheetham, G. M. T., and Steitz, T. A. (1999) *Science 286*, 2305−2308.
8. Jeruzalmi, D., and Steitz, T. A. (1998) *EMBO J. 17*, 4101−4113.
9. Patel, S. S., Wong, I., and Johnson, K. A. (1991) *Biochemistry 30*, 511−525.
10. Kiefer, J. R., Mao, C., Braman, J. C., and Beese, L. S. (1998) *Nature 391*, 304−307.
11. Li, Y., Korolev, S., and Waksman, G. (1998) *EMBO J. 17*, 7514−7525.
12. Doublie, S., Tabor, S., Long, A. M., Richardson, C. C., and Ellenberger, T. (1998) *Nature 391*, 251−258.
13. Doublié, S., and Ellenberger, T. *Curr. Opin. Struct. Biol. 6*, 704−712.
14. Sousa, R. (1996) *Trends Biochem. Sci. 21*, 186−190.
15. Steitz, T. A. (1998) *Nature 391*, 231−232.
16. Johnson, K. A. (1993) *Annu. Rev. Biochem. 62*, 685−713.
17. Orlova, M., Newlands, J., Das, A., Goldfarb, A., and Borukhov, S. (1995) *Proc. Natl. Acad. Sci. U.S.A. 92*, 4596−4600.
18. Izban, M. G., and Luse, D. S. (1992) *Genes Dev. 6*, 1342−1356.
19. Sastry, S. S., and Ross B. M. (1997) *J. Biol. Chem. 272*, 8644−8652.
20. Bonner, G., Patra, D., Lafer, E. M., and Sousa, R. (1992) *EMBO J. 11*, 3767−3775.
21. Komissarova, N., and Kashlev, M. (1998) *Proc. Natl. Acad. Sci. U.S.A. 25*, 14699−14704.
22. Gopal, V., Brieba, L. G., Guajardo, R., McAllister, W. T., and Sousa, R. (1999) *J. Mol. Biol. 290*, 411−413.
23. Huang, J., Villemain, J., Padilla, R., and Sousa, R. (1999) *J. Mol. Biol. 293*, 457−475.
24. Guajardo, R., Lopez, P., Dreyfus, M., and Sousa, R. (1998) *J. Mol. Biol. 281*, 777−792.
25. Huang, Y., Beaudry, A., McSwiggen, J., and Sousa, R. (1997) *Biochemistry 36*, 13718−13728.
26. Martin, C. T., Muller, D. K., and Coleman, J. E. (1998) *Biochemistry 27*, 3966−3974.
27. He, B., Minqing Rong, M., Durbin, R. K., and McAllister, W. T. (1997) *J. Mol. Biol. 265*, 275−288.
28. Ikeda, R. A., and Richardson, C. C. (1987) *J. Biol. Chem. 262*, 3790−3799.
29. Remington, K. M., Bennett, S. E., Harris, C. M., Harris, T. M., and Bebenek, K. (1998*) J. Biol. Chem. 273*, 13170−13176.
30. Minnick, D. T., Bebenek, K., Osheroff, W. P., Turner, R. M., Jr., Astatke, M., Liu, L., Kunkel, T. A., and Joyce, C. M. (1999) *J. Biol. Chem. 274*, 3067−3075.
31. Kommisarova, N., and Kashlev, M. (1997) *Proc. Natl. Acad. Sci. U.S.A. 94*, 1755−1760.
32. Bonner, G., Lafer, E. M., and Sousa, R. (1994) *J. Biol. Chem. 42*, 25120−25128.
33. Patra, D., Lafer, E. M., and Sousa, R. (1992) Isolation and Characterization of Mutant Bacteriophage T7 RNA Polymerases. *J. Mol. Biol. 224*, 307−318.
34. Gardner, L. P., Mookhtiar, K. A., and Coleman, J. E. (1997) *Biochemistry 36*, 2908−2918.
35. Minick, D. T., Astatke, M., Joyce, C. M., and Kunkel, T. A. (1996) *J. Biol. Chem. 271*, 24954−24961.
36. Bebenek, K., Beard, W. A., Casa-Finet, J. R., Kim, H.-R., Darden, T. A., Wilson, S. H., and Kunkel, T. A. (1995) *J. Biol. Chem. 270*, 19516−19523.
37. Osheroff, W. P., Beard, W. A., Wilson, S. H., and Kunkel, T. A. (1999) *J. Biol. Chem. 274*, 20749−20752.
38. Levin, J. R., and Chamberlin, M. J. (1987) *J. Mol. Biol. 196*, 61−84.
39. Karasavas, P., Chin-Bow, S. T., Sousa, R., and McAllister, W. T. (submitted for publication).

BI000579D